Numerical Simulations of Soft and Hard Turbulence: Preliminary Results for Two-Dimensional Convection

E. E. DeLuca, J. Werne, and R. Rosner
Enrico Fermi Institute, The University of Chicago, Chicago, Illinois 60637

F. Cattaneo
Joint Institute for Laboratory Astrophysics, University of Colorado, Boulder, Colorado 80309
(Received 8 January 1990)

We report results on the transition from soft to hard turbulence in simulations of 2D Boussinesq convection. The computed probability densities for temperature fluctuations are exponential in form in both soft and hard turbulence, unlike what is observed in experiments; in contrast, we obtain a change in the Nusselt number scaling on Rayleigh number in good agreement with the 3D experiments.

PACS numbers: 47.25.Cg, 47.25.Qv

It has been recognized for some time that Rayleigh-Bénard convection provides an excellent model for studying the onset of chaotic behavior, with the experiments of Heslot, Castaing, and Libchaber[1] providing some of the best examples of the transition to turbulence from laminar regimes. These experiments were perforce carried out in three-dimensional (3D) cells (containing either water or gaseous helium); on the theoretical side, much of our understanding of the transition to turbulence in such systems has been developed on the basis of 3D models.[2] The work reported in this Letter is motivated by studies of the scaling behavior of the dimensionless heat flux (Nu) on the Rayleigh number (R) in turbulent convection, and of the statistical properties of temperature fluctuations under such circumstances.[3] Our aim is to demonstrate that the most striking aspects of these studies can be captured by simulations of Rayleigh-Bénard convection in 2D, suggesting that 3D behavior is not necessarily required to recover either the statistical properties of temperature fluctuations in the "hard"-turbulent regime, or the reported dramatic change in the power-law dependence of the convective heat flux (Nu -1) on Rayleigh number.[3]

The formation of plumes on the thermal boundary layer has been associated with the transition from classical or "soft" turbulence to hard turbulence.[3] The onset of these plume, or "blob," instabilities have been studied in both 2D and 3D.[4-6] In our 2D simulations, conducted at Prandtl number (σ) 7 and for R between 10^6 and 1.6×10^8, the plume instability is the first instability to be realized from the steady-state roll. The instability is absent for $\sigma \leq 1$.[7] The instability sets in as a wave on the thermal boundary layer: As R is increased, plumes emerge from these waves and are advected around the cell; the time scale for the oscillatory convection is just the turnover time.

Our numerical technique is based on a pseudospectral Fourier-Chebyshev "tau" method[8] applied to the Boussinesq equations for thermal convection. [The Boussinesq approximation[9] assumes density fluctuations are unimportant everywhere except in the buoyancy term. The fluid is therefore taken to be incompressible, with constant coefficients of expansion (α), viscosity (ν), and thermal conductivity (κ).] The vertical dependence of the temperature, velocity, and pressure is represented by Chebyshev polynomials, while the horizontal dependence is expanded in sine or cosine series; the number of modes used in each simulation is given in Table I. The 2D simulations are computed in a box of unit aspect ratio, with no slip, fixed temperature boundary conditions at the top and bottom, and impenetrable ($V_{\rm perp}=0$), free-slip, insulating sidewalls. Three-dimensional calculations were also carried out using the same boundary conditions, the major difference being the aspect ratio ($1:\frac{1}{2}:1$) of the rectangular box. Boundary conditions on the pressure are computed by the influence-matrix method.[8,10] Implicit Crank-Nicolson time integration is used to advance the diffusive terms, while the nonlinear and forcing terms are explicitly advanced by a three-level Adams-Bashforth scheme. In order to compare with the experiments of Heslot, Castaing, and Libchaber,[1] we have explored a range in σ and R in both 2D and 3D. In this Letter, we limit our discussion to the turbulent 2D solutions ($R \geq 1.28\times10^6$, $\sigma=7$). Reference will be made to the other 2D and 3D solutions wherever a comparison is illuminating.

The discovery of a new state of convective turbulence by Heslot, Castaing, and Libchaber has profound implications for our understanding of turbulence. The new state of hard turbulence has been distinguished from soft turbulence in two ways: First, the probability distributions of the temperature fluctuations have Gaussian form in the soft-turbulence state, and an exponential form in the hard-turbulence state. Second, the power-law dependence of Nu -1 on R is significantly different for the two regimes: The classical state has an exponent of $\frac{1}{3}$, while the hard-turbulence state has an R exponent of $\frac{2}{7}$. Our results, on the other hand, suggest that the primary dis-

TABLE I. The basic data summarizing our simulations. R is Rayleigh number ($R_c = 1\,708$); *resolution* is the number of sines or cosines used in the horizontal direction, and the number of Chebyshev polynomials used in the vertical direction (our aspect ratio is always 1); Nu is Nusselt number, averaged over the entire run; *run time* is the length of the run in diffusion times (not including initial transients); the dimensionless time unit is the thermal diffusion time for half the vertical height, defined as $(L/2)^2/\kappa$, where the height and width of the computational box are both of length $L=2$ in dimensionless units; *turnover time* is the time it takes a fluid parcel to circulate around the box with the rms speed, approximately given by $4L/$(rms velocity); γ are coefficients of the best-fit exponential for the fluctuation histograms [$P(T/\Delta_c) \propto \exp(\gamma T/\Delta_c)$ for $T/\Delta_c < 0$ and $T/\Delta_c > 0$, respectively].

R	Resolution	Nu	Run time	Turnover time	γ
1.28×10^6	97	8.42	1.57	4.97×10^{-2}	1.4, −1.8
1.92×10^6	97	9.47	0.95	3.96×10^{-2}	1.3, −1.4
2.56×10^6	97	10.41	0.95	3.29×10^{-2}	1.8, −1.4
3.84×10^6	97	11.75	0.95	2.62×10^{-2}	1.4, −1.4
5.12×10^6	97	12.86	1.50	2.24×10^{-2}	1.4, −1.4
7.68×10^6	97	14.40	0.79	1.79×10^{-2}	1.3, −1.2
1.024×10^7	97	15.59	1.29	1.54×10^{-2}	1.2, −1.4
2.048×10^7	129	18.79	0.62	1.07×10^{-2}	1.4, −1.7
4.096×10^7	129	22.84	0.31	6.04×10^{-3}	1.6, −1.2
8.192×10^7	129	27.70	0.57	4.86×10^{-3}	1.5, −1.2
1.600×10^8	129	33.35	0.29	3.22×10^{-3}	1.4, −1.3

tinction between hard and soft turbulence resides in the changes in the Nu-R scaling alone; and that the appearance of temperature-fluctuation histograms with an exponential form is primarily a diagnostic for the presence of plumes within the flow, and not of a transition to a new turbulent state. Our results are consistent with both the scaling arguments of Castaing *et al.*[3] and with the recent work on limiting probability distributions.[11]

Our results may be summarized as follows: Implementation of the 2D version of our code with $\sigma=1$ and R as high as 1×10^7 results in steady-roll solutions. The thermal and viscous boundary layers at the constant-temperature boundaries remain stable, and shrink as R is increased. An increase of σ to 7 produces time-dependent behavior, setting in between $R=3.2\times10^4$ and 10^5. At $R=10^5$, the boundary-layer region appears to be unstable: Waves propagate along the boundary layer in the direction of the flow, and temperature and velocity fields are oscillatory. At $R=3.2\times10^5$, plumelike structures emitted from the boundary layer become apparent; and by $R=1\times10^7$, the flow field is dominated by plumes.

A summary of the parameters characterizing our solutions in the turbulent regime is given in Table I; and Fig. 1 shows the scaling behavior of Nu − 1 with R (normalized by the critical Rayleigh number $R_c=1708$ for our boundary conditions[12]) for the 2D simulations. We can clearly identify two regions in these plots: the lower region ($R \le 5.12\times10^6$) has a slope consistent with a $\frac{1}{3}$ power law, while the upper region ($R \ge 5.12\times10^6$) has a slope consistent with a $\frac{2}{7}$ power law. Our transition occurs at about $R=5.12\times10^6$ or about $R \approx 3000R_c$, in the helium experiments[1] the transition occurs at $R \approx 7000R_c$. We consider this to be a very good agreement considering the differences in Prandtl number ($\sigma \approx 0.7$ in the He experiments), geometry (2D vs 3D), and boundary conditions.

Based on earlier simulations in 2D and 3D,[2] it is somewhat surprising that our 2D numerical experiments

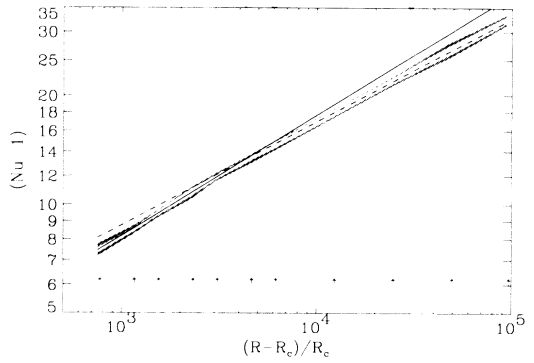

FIG. 1. Plot of the scaling of the heat flux (or Nusselt number, Nu) with the Rayleigh number (R) for our 2D simulations. The shaded regions are based on the solutions obtained by us, and listed in Table I, while the lines indicate the slopes of theoretically predicted scaling behaviors. (The solid line corresponds to a power law $\mathrm{Nu}-1 \approx [(R-R_c)/R_c]^{\alpha}$, with $\alpha=\frac{1}{3}$; the dashed line corresponds to $\alpha=\frac{2}{7}$. The normalization of these lines is arbitrary.) The lightly shaded region shows the range of variation in Nu when we average the time traces over ten turnover times; the darker-shaded region shows the correspondingly larger range of variation when we average over only five turnover times. The arrows along the bottom indicate the values of Rayleigh number for eleven simulations on which the results shown here are based.

agree so closely with the 3D experiments conducted by Heslot, Castaing, and Libchaber, and it is hence worthwhile to consider our results in more detail. Figure 2 shows the temperature-fluctuation histograms for four different values of R, superimposed on one another by rescaling the temperature with the rms temperature for the time series. (No zero-point corrections have been introduced because the time series are concatenations of "data" collected at four points equally spaced about the center of the computational cell where the mean temperature is zero.) Note especially the exponential form of the histograms as well as their universal character: For example, the histogram for $R=1.92\times10^6$ corresponds to a point that has a classical $\frac{1}{3}$ power law for the $\mathrm{Nu}-1$ vs $(R-R_c)/R_c$ scaling relation, but nevertheless here shows an exponential form. Indeed, we are unable to find temperature-fluctuation hisotgrams with Gaussian form for any value of R in the turbulent regime, in strong contrast to the experimental results. In Table I we give the best-fit coefficients γ of the temperature-fluctuation hisotgrams to an exponential form. These values γ are very close to the value predicted by Yakhot,[11] and somewhat larger than those seen in the experiments, as well as in the 3D simulations by Sirovich, Balachander, and Maxey.[13] The scatter in our best-fit exponent is due to the combination of short-time strings (when compared with the experiments) and few sampling points (when compared with the simulations with periodic side walls[13]). We cannot sensibly combine all of our horizontal data points to obtain better statistics because the flow is only isotropic in the very center of our box. We further note that the corresponding velocity histograms are Gaussian in form. Unfortunately, the experiments cannot easily measure velocity fields, but such measurements would be invaluable to the construction of a theoretical explanation for these turbulent flows.

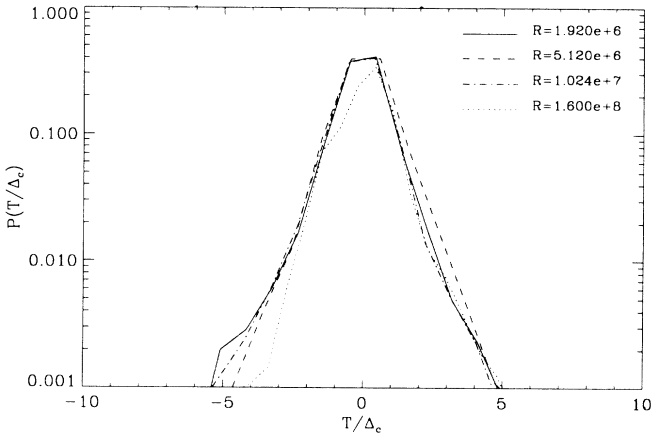

FIG. 2. Frequency histograms of the temperature-fluctuation amplitudes for four different values of R. Note the universal character of these exponentially shaped distributions, despite the fact that for the lowest value of R, experiments in 3D indicate distributions with Gaussian form.

Why is it that our 2D code is able to produce some of the features of the experimental results and not others? Recall that our computations are performed with rigid, no-slip boundaries at the top and bottom, and rigid, *free-slip* boundaries on the vertical walls. With these boundary conditions, we are unable to form counter rolls in the corners of the box; and for what follows, it is important to recall that instabilities associated with these counter rolls are known to give rise to time-dependent convection at R *lower* than the onset of the plume instability discussed above.[14]

A possible explanation of the discrepancy between our results and the experimental results is as follows: The exponential form of the temperature-fluctuation histograms is known to arise from the advection of plumes, and plume fragments, past the probes in the box.[3] Hence, whenever the boundary layer becomes unstable to the formation of plumes, we would expect histograms of an exponential form to arise.[11] However, the mere presence of plumes is insufficient to change the form of the $\mathrm{Nu}-1$ vs $(R-R_c)/R_c$ scaling behavior: The plumes must exceed some threshold of vigor and/or frequency in order to modify the structure of the flow to the point of affecting the overall heat flux. We know from other simulations (including our 3D simulations) that nonplumelike instabilities do lead to temperature-fluctuation histograms with Gaussian form, and we expect that any such instabilities in the present case would lead to similar distribution functions, at least until the plume instability is sufficiently vigorous so as to modify the flow. Thus, in 3D, with similar boundary conditions to the 2D case considered here, time dependence arises first from a sausage instability,[2,4] only after which the boundary layer becomes unstable to plumes; the temperature-fluctuation histogram has Gaussian form in this 3D case as long as the sausage instability predominates. In the present case, there are no instabilities which can compete with the plume instability, especially for R below that for the onset of the plume instability; and hence we do not expect to find temperature-fluctuation histograms with a functional form other than exponential.

In conclusion, we have found a transition from soft to hard turbulence in numerical simulations of 2D Boussinesq convection, marked by a change in the Nu scaling on R from a $\frac{1}{3}$ to a $\frac{2}{7}$ power-law index. This change is, however, not accompanied by a change in form of the temperature-fluctuation histograms; our histograms show exponential form throughout both the soft- and hard-turbulence regimes. We interpret this result as a consequence of the absence of instabilities in our 2D case which can compete with the plume instability. We therefore believe that it is solely the scaling of Nu on R which determines whether one is in the soft- or hard-turbulence regime. Our results also show the velocity-fluctuation histograms for the 2D case to be Gaussian for all the turbulent solutions; this result is as yet not verified experimentally.

We appreciate comments on our work by A. Libchaber and L. Kadanoff. This work was supported in part by NASA grants to The University of Chicago. We acknowledge the generous computing support of the Argonne National Laboratory.

[1]F. Heslot, B. Castaing, and A. Libchaber, Phys. Rev. A **36**, 5870 (1987).

[2]R. M. Clever and F. H. Busse, J. Fluid Mech. **65**, 625 (1974); F. M. Busse and R. M. Clever, J. Fluid Mech. **91**, 319 (1979).

[3]B. Castaing, G. Gunaratne, F. Heslot, L. Kadanoff, A. Libchaber, S. Thomae, X. Z. Wu, S. Zaleski, and G. Zanetti, J. Fluid Mech. **204**, 1 (1989).

[4]E. W. Bolton, F. H. Busse, and R. M. Clever, J. Fluid Mech. **164**, 469 (1986).

[5]D. R. Moore and N. O. Weiss, J. Fluid Mech. **58**, 289 (1973).

[6]T. B. Lennie, D. P. McKenzie, D. R. Moore, and N. O. Weiss, J. Fluid Mech. **188**, 47 (1988).

[7]J. H. Curry, J. R. Herring, J. Loncaric, and S. A. Orszag, J. Fluid Mech. **147**, 1 (1984).

[8]C. Canuto, M. Y. Hussaini, A. Quarteroni, and T. A. Zang, *Spectral Methods in Fluid Dynamics* (Springer-Verlag, New York, 1988).

[9]E. A. Spiegel and G. Veronis, Astrophys. J. **132**, 716 (1960).

[10]L. Kleiser and U. Schumann, in *Proceedings of the Third Gesellschaft für Angewandte Mathematik und Mechanik Conference Numerical Methods in Fluid Mechanics,* edited by E. H. Hirschel (Vieweg, Braunschweig, 1980), p. 165.

[11]Ya. G. Sinai and V. Yakhot, Phys. Rev. Lett. **63**, 1962 (1989); V. Yakhot, Phys. Rev. Lett. **63**, 1965 (1989).

[12]S. Chandrasekhar, *Hydrodynamic and Hydromagnetic Stability* (Oxford Univ. Press, Oxford, 1961).

[13]L. Sirovich, S. Balachandar, and M. R. Maxey, Phys. Fluids A **1**, 1911 (1989).

[14]I. Goldhirsch, R. B. Pelz, and S. A. Orszag, J. Fluid Mech. **199**, 1 (1989).